

HIGH PRODUCTIVITY WELDING OF A MODERN HIGHER NIOBIUM, LOW CARBON PIPE STEEL FOR HIGH TOUGHNESS APPLICATIONS

S. Starck¹ & D.S. Taylor²

¹ Oerlikon Schweisstechnik GmbH;
Industriestrasse 12, Eisenberg /Pfalz, 67304, Germany

² Air Liquide Welding;
13, rue d'Epluches, Saint Ouen l'Aumône, Cergy Pontoise, 95315, France

Keywords: Microalloying, Linepipe, Higher Niobium, High Toughness Weld Metal, HSLA Materials, CTOD, Weldability, Multi-wire Submerged Arc Welding, Pipeline Welding

Abstract

A new generation higher niobium X70 pipe steel has been welded using the high productivity submerged arc, multi-wire process with 2 passes for joining the longitudinal seams. High toughness weld deposits have been produced using a microalloying system produced using solid TiB SAW welding wires combined with a specially designed semi-basic SAW flux. High levels of toughness were produced in the weld metal and heat affected zone, evaluated using ISO-V and CTOD testing.

Introduction

As the demand for liquid natural gas (LNG) increases, so do the requirements for more efficient gas transport. One method is the use of high pressure pipelines; the normal European grid is pressurised at 80 bar, but it is considered feasible to increase the pressure to 100 bar or 150 bar maximum, as an offshore pipeline, by decreasing the number of compression stations, which is very cost effective. This requires thicker and/or stronger pipe steels, to API grade X80 and possibly to X100 depending on design considerations.

Higher strength pipe steels are required for long distance land pipelines in > 40 in diameter, as larger diameter pipe lines reduce transport friction and thinner wall sections facilitate more efficient laying.

Offshore lines are currently predominantly X65 and increased use of higher strength levels through X70 to X80 is forecast, however it is considered unlikely that the strength level of X80 will be exceeded, due to pipe buckling considerations during laying.

A new generation of steels has been developed for higher strength linepipe using a higher niobium and low carbon lean alloying system [1]. This alloying regime is used to produce high strength, high toughness steels via thermo-mechanical steel processing routes while maintaining low carbon and hence low carbon equivalent values, resulting in good weldability and HAZ toughness properties. This alloying system is cost effective and alloying with nickel is minimised. The weldability of a steel for linepipe applications from this new generation of pipe steels has been investigated, specifically for high productivity longitudinal pipe seam welding using the two pass submerged arc welding (SAW) multi-wire process.

Pipe Steel

The plate used in this programme conforms to X70 grade, supplied from the HIPERC project or high performance, economic steel concept for line pipe and general structural use, funded by the EU Research Fund for Coal and Steel (RFCS). The plate chemical composition and mechanical properties are reported in Table I. The same plate chemistry could be finished to X80 or thick section X65, depending on the steel processing route selected.

Table I. Plate Chemical Composition and Mechanical Properties

C	Si	Mn	P	S	Al	Nb	V	Cu
0.053	0.18	1.59	0.013	0.0038	0.037	0.097	0.001	0.23
Cr	Ni	N	Mo	Ti	Ca	B	Pcm	CEV
0.26	0.17	0.006	0.002	0.016	0.0013	-	0.17	0.40

(wt.%)

Product ID	Slab size (mm)	Transfer bar thickness (mm)	SRT (°C)	EHT (°C)	FRT (°C)	Plate thickness (mm)	Reduction ratio	Processed to pipe ID	Pipe outer diam. (mm)
PB329	230 x 1970	86.3	1236	798	708	20.9	4.1	YBRP2	914

Product ID	Product	t (mm)	RR	FRT (°C)	R t0.5 (MPa)	Rm (MPa)	A (%)	Rt/Rm	27 J ITT (°C)	0.5 Kv max ITT (°C)	DWTT (°C)
PB329	Plate	20.9	4.1	708	533	592	18	0.90	-100	-85	-40

The microalloying system of this plate is 0.097% niobium, low carbon 0.053% with intermediate nitrogen of 60 ppm. The function of the low carbon is to ensure that toughness in the HAZ is retained, the Nb/C/N function being to precipitation strengthen the matrix and for grain size management, supported by the solid solution elements Mn, Cr and Ni to increase hardenability while ensuring lower temperature transformation products when welding. The Nb in solution will also delay the austenite to ferrite phase transformation.

Welding Programme

Ten higher niobium plates from the HIPERC project, plate size 20 mm x 1000 mm x 2000 mm, were welded by Air Liquide Welding Germany with a commercially available SAW wire and flux combination designed specifically for high strength, high toughness welding of line pipe steels. A high productivity welding procedure was used, which is typical of that used industrially in modern pipe mills for the two pass longitudinal seam welding of pipes for gas transportation and offshore applications.

No pre-heat was applied before welding. The internal seams were welded using 4 x 4 mm SAW wires (DC-AC-AC-AC) at a welding speed of 1.60 m/min and a combined heat input of

4.1 kJ/mm. The external seams were welded using 5 x 4 mm SAW wires (DC-AC-AC-AC-AC) at a welding speed of 2.15 m/min and a combined heat input of 4.4 kJ/mm.

Welding Consumable Requirements & Selection

Longitudinal pipe welding with the two pass submerged arc welding process, using 5 x 4 mm wires for the outside seam and 4 x 4 mm wires for the inside seam, is a high speed, very high deposition rate process. Combined cumulated welding currents of 5,000 A are typical, with welding speeds of 2.5 m/min and faster, at heat inputs nominally in the range 4-5 kJ/mm, depositing > 40 kg/hour of weld metal. This is a very high dilution welding process, with typical levels of weld metal dilution of 70% and a demanding process for both weld metal and HAZ mechanical properties, due to the high levels of heat input and the consequent peak temperatures and subsequent thermal cycle.

The demands on the SAW welding flux are high [2], requiring:

For welding process considerations [3]:

- High tolerance to welding currents, operation at 1,500 A is a possible requirement for thicker pipe sections >25 mm.
- Ability to weld at high welding speeds, > 2 m/min, while retaining arc stability.
- Stable grain size distribution following re-cycling (grain strength and toughness).
- Self releasing slag.
- A smooth and even finished weld bead profile without excessive reinforcement, requiring no dressing, with well blended weld toes without undercut.

For metallurgical considerations [4]:

- Low moisture content/diffusible hydrogen < 5 ml/100 g deposited weld metal (to minimise pre-heat).
- Low rate of moisture pick up during use (to prevent hydrogen induced “cold” or chevron cracking).
- Oxygen content and element transfer characteristics specifically tailored to microalloyed wires.
- High resistance to copper induced cracking.
- NDT cleanliness.
- Resultant weld metal system which is tolerant to niobium dilution in the range 0.05-0.06%.

The SAW flux designed to meet these criteria is a commercially available aluminate-basic agglomerated type, OERLIKON OP 132, with a Boniszewski basicity index of 1.5 which has been specifically designed for these demanding pipe welding applications. The chemical constituents are given in Table II.

Table II. Chemical Composition of the SAW Flux

CaO + MgO	CaF ₂	Al ₂ O ₃ + MnO	SiO ₂ + TiO ₂
23%	15%	35%	20%

During welding, this SAW flux donates manganese and is silicon neutral. The element transfer characteristics of OP 132 are shown in Figure 1.

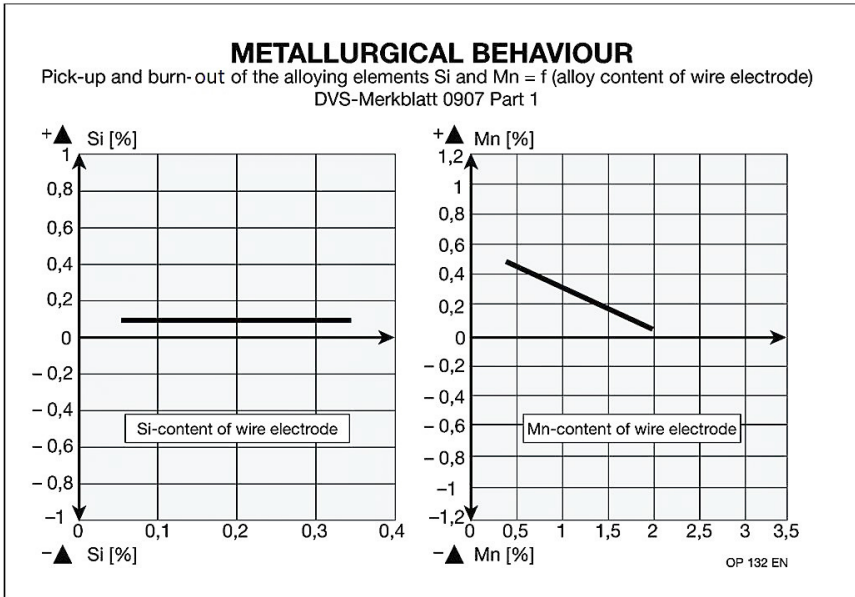


Figure 1. SAW flux transfer characteristics.

The microstructure of the weld deposit must deliver not only the strength level required, but more challenging is generating the required levels of fracture toughness in the as-welded condition. High levels of weld metal toughness are produced by microstructures with high levels of fine acicular ferrite with a very low volume fraction of grain boundary ferrite.

To achieve these microstructures, transformation at the austenite grain boundaries must be delayed, nucleation of ferrite at these sites inhibited and the intra granular nucleation of acicular ferrite on multiple inclusion sites promoted. Networks of pro-eutectoid ferrite outlining the prior austenite grain boundaries must be suppressed or eliminated.

In practice, when welding the longitudinal seams of linepipe using SAW multi-wire, C-Mn-Mo-Ti-B SAW wires are used with semi-basic SAW fluxes [2, 4, 5]. This system can be optimised to produce micro-alloyed weld metal of sufficient hardenability, derived from the wire chemistry/ies, at the required oxygen level of the system to produce an appropriate volume fraction and size distribution of inclusions, derived from the SAW flux.

Testing Programme

The testing programme [6] was designed to investigate weld metal, HAZ and plate fracture toughness after welding and to correlate these results with microstructure, hardness surveys and precipitation in the weld metal.

Mechanical Property Assessments

Weld Metal Tensile Testing. Three tensile test specimens were taken from the weld metal centre line at the plate centre line. (Specimen diameter 7.92 mm, cross sectional area 49.27 mm², gauge length 40 mm.)

Charpy-V Impact Testing. Specimens were taken from the weld metal at the centre line of the weld beads at three plate locations, see Figure 2, 2 mm below the top, outer, surface (S), plate centre line (C) and 2 mm below the bottom, inner, surface (I). Weld metal specimens were tested at 0 °C, -20 °C, -40 °C & -60 °C.

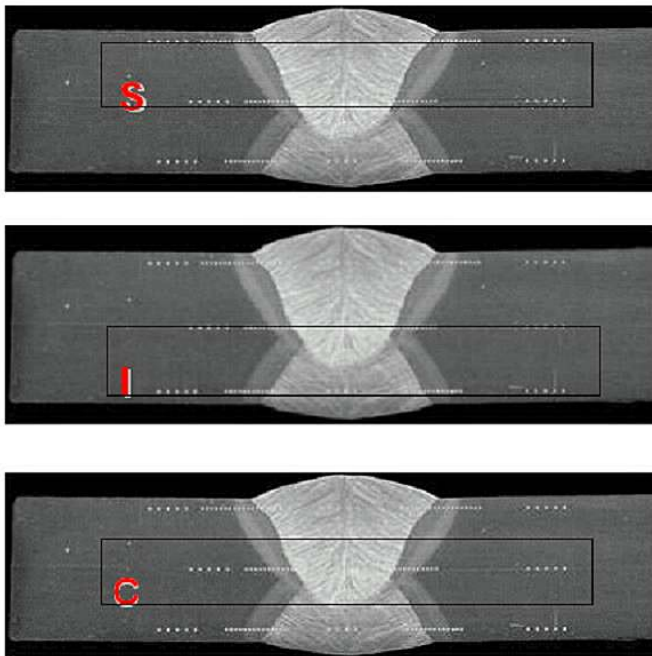


Figure 2. Charpy-V weld metal test locations.

Charpy-V specimens were also taken at the fusion line (FL), FL+2 mm and FL+5 mm for testing at 0 °C & -20 °C.

CTOD Testing. Fracture mechanics properties were evaluated using single edge notch bend (SENB) $B \times 2B$ specimens, see Figure 3, with a through-thickness notch sampling the heat affected zone and the fusion line.

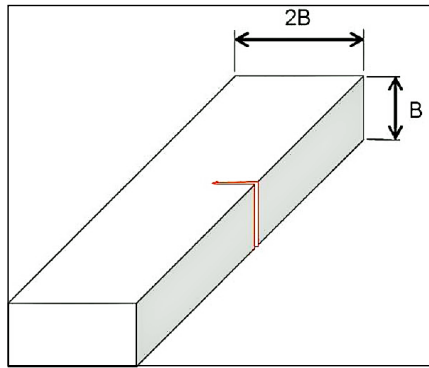


Figure 3. SENB Specimen characteristics.

The notch locations were all 50% base material and 50% weld material, see Figure 4.

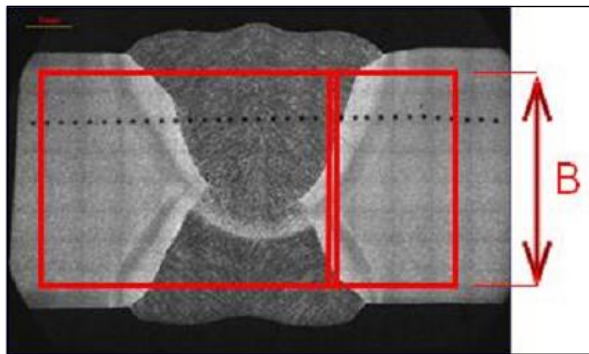


Figure 4. Notch location in SENB specimen.

Specimens were notched by electrical discharge machining (EDM) – radius $R = 0.5$ mm with a target notch depth of $a/W = 0.5$, fatigue pre-cracking growth included.

Specimens were tested at 3 temperatures, 0 °C, -10 °C and -20 °C with the test examination in accordance with ASTM E1820-09, multi-point single specimen technique.

Crack tip opening displacement (CTOD) was evaluated according to fracture toughness standards BS 7448 and ASTM E1820-01 with the critical CTOD fracture parameter obtained by load vs. COD curve at final load displacement.

Microstructure, Hardness and Precipitation

Metallographic Evaluation of the Weld, HAZ, FL and parent plate was carried out by optical microscopy and scanning electron microscopy (SEM) and the electron back scattered diffraction (EBSD) technique.

Hardness Surveys were performed at three locations. Location B at mid thickness, location C at 1.5 mm from the top surface and location A at 1.5 mm from the bottom surface, Figure 5.

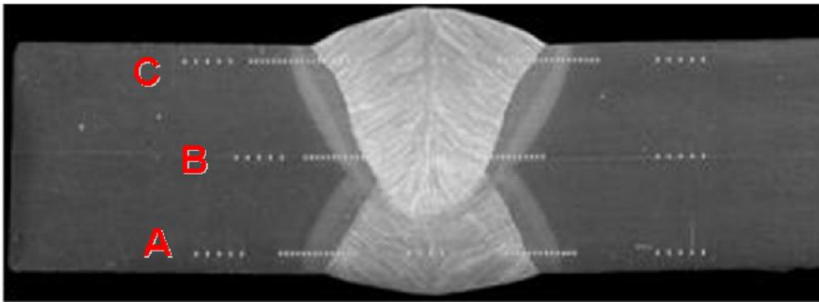


Figure 5. Hardness survey locations.

Chemical Determinations of the base plate, welding wire and weld deposit for C, Mn, Si, S, P, Ni, Cr, Mo, Nb, Cu, V, Ti, and B were made using spark emission spectroscopy, N by thermal conductivity and O by infrared spectroscopy.

Oxygen Content in the Weld Metal was also determined by metallographic method (SEM+EDS). Oxide volume fraction was measured by automatic image analysis.

Precipitate Analyses in the Base Metal were investigated using TEM on extraction replicas.

Results

Mechanical Property Assessments

Weld Metal Tensile Strength Results are shown in Table III. The tensile strength of the weld metal is 720 MPa, which comfortably overmatches the base plate to the strength level required for X80.

Table III. Weld Metal Strength Results

Yield strength (MPa)	Tensile strength (MPa)	Elongation (%)	Reduction of area (%)
653	720	21	70

Charpy-V Impact Toughness Testing results are shown in Tables IV.

The specimens notched in the *weld metal* showed consistently high levels of weld deposit toughness at all three testing locations down to -60 °C, see Table IV-1. Fracture surfaces were fully ductile in all 3 locations to -20 °C.

At location (I), the inner seam, upper shelf toughness is retained to -20 °C, 176 J to 198 J. The weld metal enters transition at temperatures below -20 °C, however, a high level of toughness is retained at -60 °C, 108 J to 130 J.

At location (C), the plate centre line, upper shelf toughness is retained to -40 °C, 168 J to 192 J. The weld metal enters transition at temperatures below -40 °C, however, a high level of toughness is retained at -60 °C, 150 J to 177 J. This is the area of highest weld metal toughness, reflecting the effect of weld tempering by the second pass.

At location (S), the outer seam, upper shelf toughness is retained to -20 °C, 176 J to 198 J. The weld metal enters transition at temperatures below -20 °C, however, a high level of toughness is retained at -60 °C, 112 J to 138 J.

Table IV-1. Charpy-V Testing Results (Weld Metal)

Energy (J)		Brittle %	Test temperature (°C)	Specimen location
	Ave.			
186	186	0	0	Position C
186		0	0	Position C
176	189.3	0	-20	Position C
198		0	-20	Position C
194		0	-20	Position C
176	167.3	0	-40	Position C
160		15	-40	Position C
166		15	-40	Position C
108	119	40	-60	Position C
130		25	-60	Position C
192	193.0	0	0	Position I
194		0	0	Position I
196	194.7	0	-20	Position I
198		0	-20	Position I
190		0	-20	Position I
168	181.3	10	-40	Position I
184		0	-40	Position I
192		0	-40	Position I
150	163.5	20	-60	Position I
177		0	-60	Position I
184	170	0	0	Position S
156		0	0	Position S
178	173.7	0	-20	Position S
175		0	-20	Position S
168		0	-20	Position S
168	155.3	0	-40	Position S
152		15	-40	Position S
146		15	-40	Position S
138	125	20	-60	Position S
112		30	-60	Position S

The specimens notched at the *fusion line*, Table IV-2, were almost fully ductile at 0 °C with high levels of upper shelf toughness. At -20 °C, entry into transitional behaviour is evident with 50-60% brittle fracture surfaces and a Cv energy of > 43 < 128 J representing lower but still acceptable levels of toughness.

The specimens notched at the fusion line +2 mm were almost fully ductile with Cv energies in the range > 204 < 264 J and at fusion line +5 mm were fully ductile with Cv energies in the range > 246 < 283 J.

Table IV-2. Charpy-V Testing Results (Fusion Line)

Notch position	Test temperature (°C)	Energy absorbed (J)		Fracture surface brittle (%)
		Individual	Average	
Fusion line	0	217	255.3	20
		277		0
		272		0
	-20	128	86.3	50
		43		60
		88		50
Fusion line + 2 mm	0	230	225.3	10
		228		10
		218		20
	-20	264	235.3	20
		204		0
		238		0
Fusion line + 5 mm	0	268	277.7	0
		283		0
		238		0
	-20	273	259.0	0
		246		0
		258		0

The weld metal upper shelf toughness values are lower than base plate upper shelf toughness values due to differences in the nature and dispersion of inclusions in the weld metal and parent plate.

Fracture Mechanics Properties. SENB testing results are shown in Table V.

Table V. Fracture Mechanics Properties: CTOD Testing

Critical Fracture Toughness						
Specimen ID	a_0/W	δ max (CTOD)	Minimum δ CTOD min	Average δ CTOD av	Temp.	Behaviour
		(mm)	(mm)	(mm)	(°C)	
SENB1	0.430	1.742	0.961	1.280	0	m-behaviour
SENB2	0.437	1.333			0	m-behaviour
SENB3	0.419	1.083			0	c-behaviour
SENB4	0.448	0.961			0	c-behaviour
SENB5	0.428	0.888	0.649	0.769	-10	c-behaviour
SENB6	0.446	0.649			-10	c-behaviour
SENB7	0.433	0.595	0.511	0.553	-20	c-behaviour
SENB8	0.444	0.511			-20	c-behaviour

The SENB applied loads vs. CMOD curves, with photographs of the fractured specimens, are shown in Figures 6a – 6d.

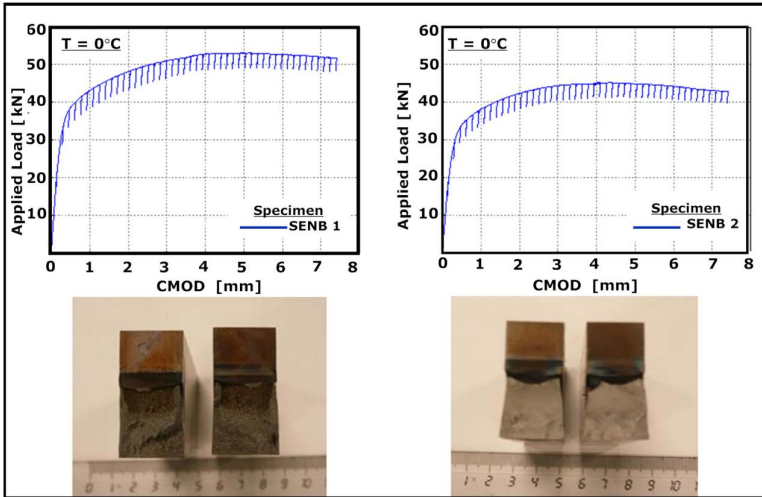


Figure 6a. Fracture mechanics properties: SENB Specimens 1 & 2.

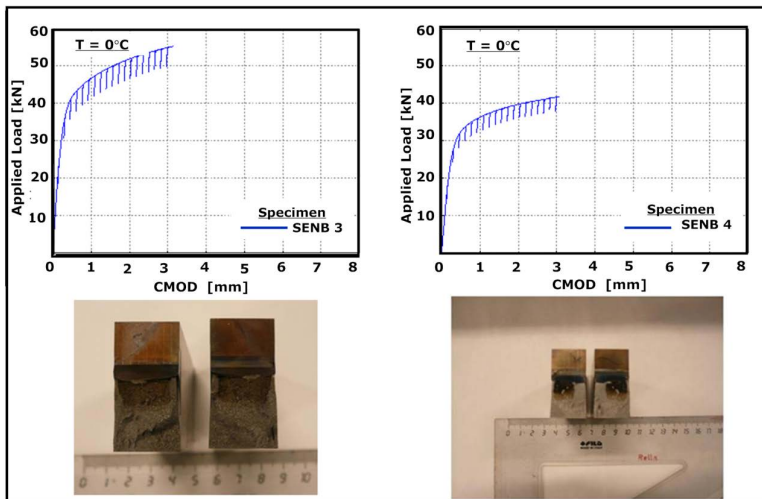


Figure 6b. Fracture mechanics properties: SENB Specimens 3 & 4.

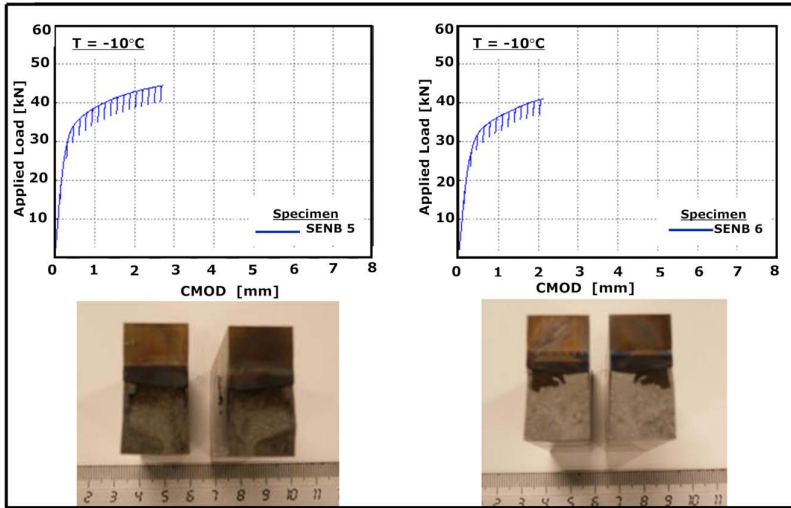


Figure 6c. Fracture mechanics properties: SENB Specimens 5 & 6.

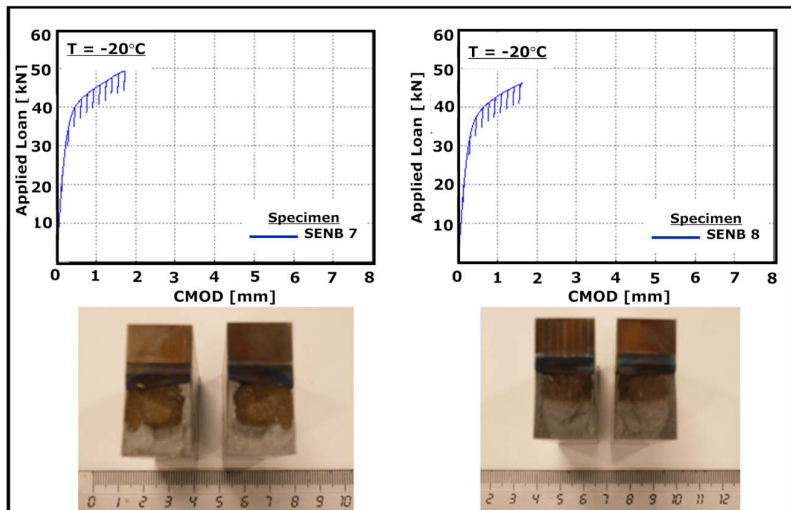


Figure 6d. Fracture mechanics properties: SENB Specimens 7 & 8.

The critical CTOD fracture parameter was obtained by load vs. CMOD curve at final load attainment.

Testing temperature, $T = 0\text{ }^{\circ}\text{C}$

2 out of 4 specimens exhibited “m-behaviour”, i.e. fully ductile crack growth

2 out of 4 specimens exhibited “c-behaviour”, i.e. fracture instability occurred at maximum load attainment.

Testing temperature, $T = -10\text{ }^{\circ}\text{C}$

Both specimens exhibited “c-behaviour”

No significant ductile crack growth was observed before instability occurred.

Testing temperature, $T = -20\text{ }^{\circ}\text{C}$

Both specimens exhibited “c-behaviour”

No significant ductile crack growth was observed before instability occurred.

Metallographic Evaluation

There are four distinct microstructural regions, which are base plate, HAZ consisting of a fine grain zone and a coarse grain zone and then the weld metal

The microstructure of the base plate is shown in Figure 7. The microstructure consists of equiaxed grains of polygonal ferrite with islands of pearlite.

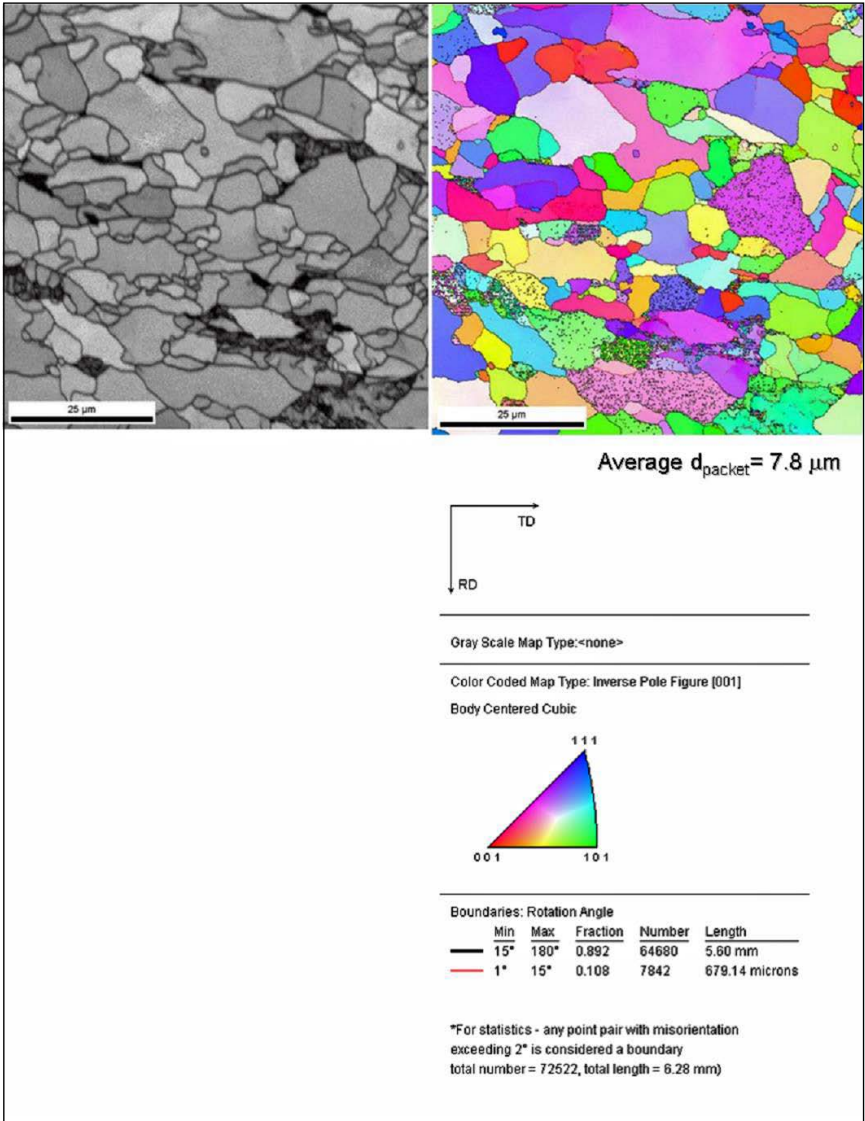


Figure 7. Base plate microstructure: optical and EBSD.

The microstructures of the fine grained zone and the coarse grained zone are shown in Figure 8. The coarse grain zone extends for about 400 μm and is shown in detail in Figure 9. The microstructure is bainite with a coarse packet size, d_{packet} is 20 μm , with a clear sub-structure.

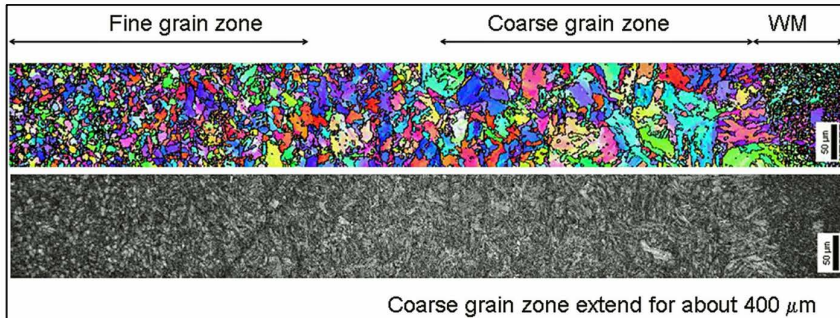


Figure 8. HAZ microstructures, fine grain zone to weld metal, optical and EBSD.

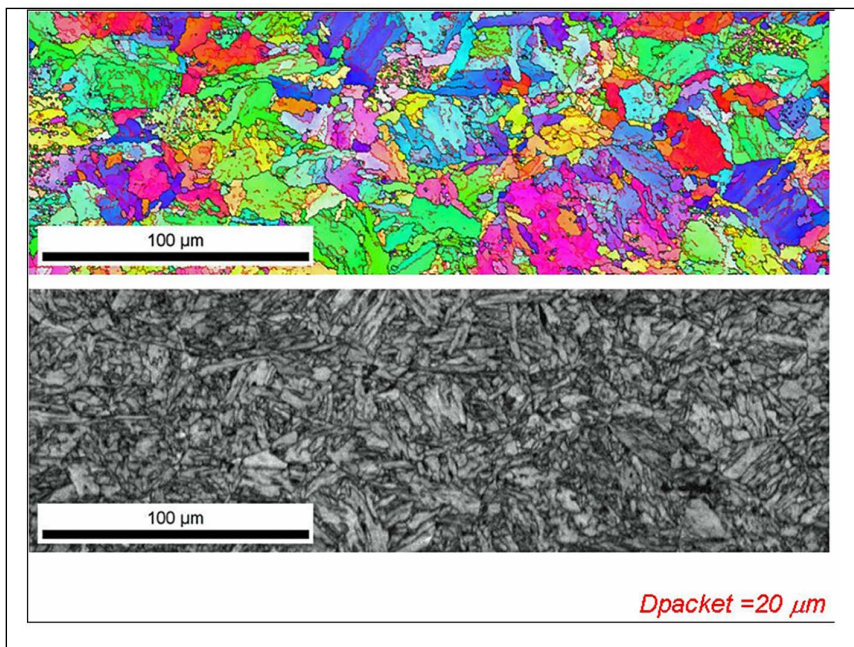


Figure 9. Microstructures, coarse grain zone detail: EBSD results.

The microstructure of the weld metal is shown in Figure 10, consisting entirely of highly refined, fine grained acicular ferrite, the microstructural constituent associated with high levels of weld metal toughness.

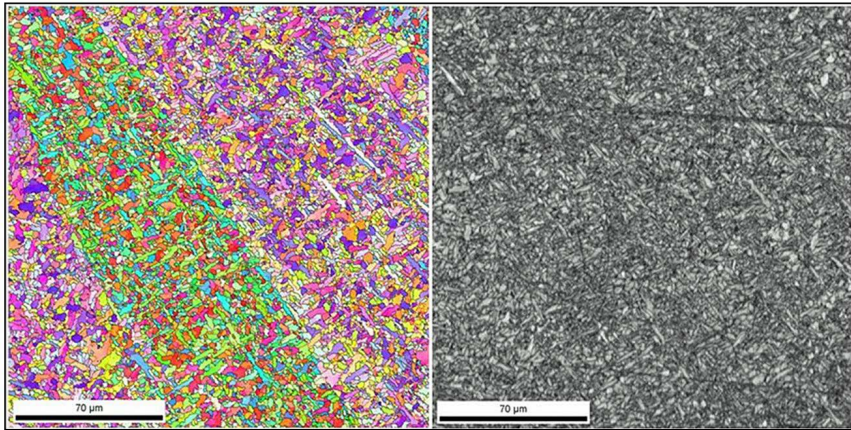


Figure 10. Microstructure, weld metal: EBSD results.

Hardness Assessment

The weld zone hardness profiles are shown in Figure 11a, 11b & 11c. The base plate hardness is 180 Hv10, which is overmatched by the weld metal hardness, 230-275 Hv10. The outer seam weld metal hardness, profile C, has a maximum hardness of 235 Hv10, while the inner seam weld metal hardness, profile A, has a maximum hardness of 275 Hv10. This difference in weld metal hardness between the two weld beads is attributed to the tempering effect of the second pass. The hardness profile across the root area of the weld (B) shows a maximum hardness of 240 Hv10, consistent with the outer seam.

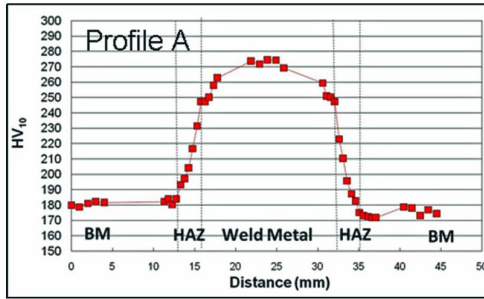


Figure 11a. Hardness survey profile A.

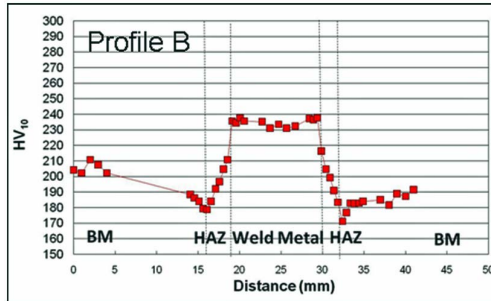


Figure 11b. Hardness survey profile B.

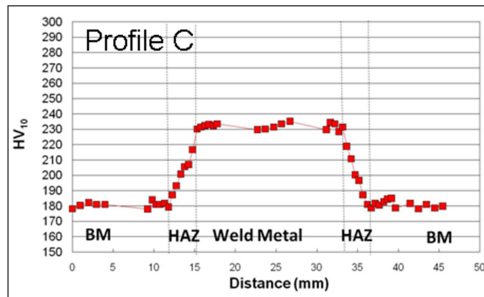


Figure 11c. Hardness survey profile C.

Chemical Determinations are shown in Table VI.

Table VI. Chemical Determinations

	(wt.%)									
	C	Mn	Si	P	S	Ni	Cr	Mo	Nb	Cu
Base metal	0.053	1.59	0.18	0.013	0.004	0.17	0.26	0.00	0.097	0.23
Wire (OE-TiBor 33)	0.077	1.25	0.31	0.009	0.003	0.02	0.03	0.53	<0.001	0.01
Weld Pos. S*	0.057	1.54	0.28	0.016	0.006	0.11	0.16	0.23	0.048	0.16
Weld Pos. C*	0.058	1.52	0.28	0.016	0.006	0.11	0.16	0.23	0.049	0.16
Weld Pos. I*	0.060	1.55	0.26	0.016	0.007	0.11	0.17	0.19	0.057	0.17

*see Figure 2

	(ppm)				
	V	Ti	B	N	O
Base metal	10	160	<5	51	27
Wire	30	1570	160	24	19
Weld Pos. S*	10	305	30	44	400
Weld Pos. C*	10	306	31	47	470
Weld Pos. I*	10	283	28	47	430

*see Figure 2

Dilution in the weld bead is ~ 60%, which is considered typical for this type of welding procedure. The nitrogen in the welding wire is low, < 50 ppm, to prevent the formation of excess TiN, as TiO and Al-Ti oxides are required, conducive with the deposit oxygen level of 400-470 ppm.

The C, Mn & Ni levels in the plate and weld deposit are similar, therefore having similar electrical potential, posing a limited risk of preferential corrosion.

The Presence of Oxides

The analyses of the oxides sampled in the weld metal are given in Table VII and the prevalent oxides are Al-Ti. The oxide volume fraction is 0.16%, representing a fine dispersion of oxides in the weld metal. Ti rich oxides are those associated with the generation of acicular ferrite, resulting in an optimum balance of weld metal toughness and hardness.

Table VII. Chemistry of Oxides in the Weld Metal

Element	Weld metal oxides			
	Weight %			
O	19.5	24.7	14.2	14.4
Al	13.0	11.6	10.2	18.9
Si	0.5	0.4	0.5	0.2
S	0.5	0.9	0.4	0.3
Ti	12.5	8.7	11.0	4.6
Mn	5.2	2.9	6.2	9.1
Fe	49.1	50.8	57.7	52.4

There are fewer, coarser oxides in the HAZ and base plate, which are predominantly Nb and Ti rich, see Figure 12.

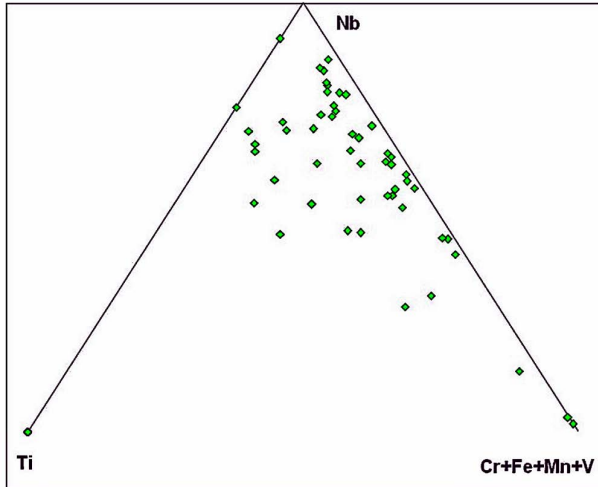


Figure 12. Precipitate chemistry in the base plate.

Discussion

Using the high productivity submerged arc multi-wire welding process with a welding procedure typical for longitudinal pipe welding, the two pass pipe welds were made at deposition rates of 78.1 and 50.5 kg/hr, for the outside and inside seams respectively, at heat inputs between 4.1 - 4.6 kJ/mm. The as-welded weld bead profiles were excellent with smooth surfaces, virtually no spatter or undercut, requiring no post weld dressing.

The fracture toughness properties of both the weld metal and HAZ were comprehensively tested.

The Charpy toughness of the weld metal, FL+2mm and FL+5mm were all fully ductile with upper shelf toughness to -20 °C. The FL showed some deterioration in toughness at -20 °C, however this was considered acceptable to prevailing fabrication requirements.

The SENB testing results, to evaluate the fracture toughness of the combined weld metal and HAZ, were excellent. Half of the specimens exhibited fully ductile “m-behaviour” at 0 °C, then “c-behaviour” at -10 °C and -20 °C, with no significant ductile crack growth before instability occurred.

Weld metal and plate optical microstructures were correlated with the toughness results obtained. The weld metal microstructure consisted of fine-grained acicular ferrite, which is consistent with the high levels of toughness. The heat affected zone microstructure of bainite with a coarse packet size is consistent with the lower toughness level, which is acceptable and could be improved with minor procedural modifications.

Conclusions

The higher Nb, low C plate from the HIPERC project evaluated in this work has demonstrated that the demanding levels of HAZ and weld metal toughness required for high pressure gas transmission lines can be achieved after welding with a high productivity industry standard welding procedure and specialised, though commercially available, welding consumables.

Further Work

A more detailed investigation of the optical microstructures and the EBSD results and chemistries in the context of the mechanical properties of the weld metal and HAZ is currently taking place. Results will be reported subsequently.

The circumferential seam weldability and HAZ properties remain to be investigated. Pipe of identical chemistry has been identified in 610 mm diameter x 14.6 mm wall. Two orbital welding processes will be investigated.

Firstly, for those production situations where the pipe is fixed and cannot be rotated, the MIG/MAG process using a multi-head automatic bug system, welding downhill with microalloyed solid fine wires, will be investigated. The joint preparation and welding procedure will be selected to be representative of current industry practice on an offshore lay barge. The welding shielding gas will use a variety of gas mixtures from the root run, welded with CO₂, through the filling passes, CO₂-Ar 60/40 and capping passes, CO₂-Ar 20/80.

Secondly, for pipe which can be rotated, SAW welding will be investigated where the joint preparation and welding procedure will be selected to be representative of current double jointing practice. In order to investigate a higher deposition rate approach, the welding procedure will also be modified to SAW twin 2.4 mm wires in a single head and twin tandem hybrid configurations.

Acknowledgements

The authors would like to thank Air Liquide Welding for permission to publish this paper. The opinions expressed are those of the authors and not necessarily those of the organisation they represent.

References

1. B. Ouaisa et al., "Investigations on Microstructure, Mechanical Properties and Weldability of a Low Carbon Steel for High Strength Helical Linepipe," *Proceedings of 17th Joint Technical Meeting Conference 2009*, Milan, Italy, (11-15 May 2009).
2. D.S. Taylor, J. Sordi and G. Thewlis, "Seam Welding Consumable Development for Critical Pipeline Service," *Proceedings of the AIM International Pipeline Technology Conference 1987*, Rome, Italy, (17-19 November 1987), 277-307.
3. B.R. Keville and B. Schlatter, "Fundamental Factors Affecting Weld Bead Shape when Using Multiple Submerged Arc Welding Systems," *Proceedings of 2nd International Pipeline Technology Conference 1995*, Ostende, Belgium, (11-14 September 1995), 1, 139-149.
4. C.E. Thornton and B.R. Keville, "Multi-Wire Submerged Arc Welding – Consumable Development," *Proceedings of 2nd International Pipeline Technology Conference 1995*, Ostende, Belgium, (11-14 September 1995), 1, 163-171.
5. J.G. Garland and P. Kirkwood, "Towards Improved Submerged Arc Weld Metal," *Metal Construction*, (May 1975), 275-283.
6. A. Di Schino, M. Guagnelli and G. Melis, "Seam Weld Assessment" (CSM report, November 2010).